Measuring Thermal Rupture Force Distributions from an Ensemble of Trajectories

J. W. Swan, M. M. Shindel, and E. M. Furst

Phys. Rev. Lett. **109**, 198302 — Published 8 November 2012

DOI: 10.1103/PhysRevLett.109.198302

Measuring thermal rupture force distributions from an ensemble of trajectories

J. W. Swan, M. M. Shindel* and E. M. Furst†
Department of Chemical and Biomolecular Engineering, Center for Molecular and Engineering Thermodynamics, University of Delaware, Newark, DE 19716, USA

Rupture, bond breaking or extraction from a deep and narrow potential well requires considerable force while producing minimal displacement. In thermally fluctuating systems, there is not a single force required to achieve rupture but a spectrum as thermal forces can both augment and inhibit the bond breaking. We demonstrate measurement and interpretation of the distribution of rupture forces between pairs of PMMA particles bonded strongly via the van der Waals attraction. The otherwise irreversible bond is broken by pulling the particles apart with optical tweezers. We show that an ensemble of the particle trajectories before, during and after the rupture event may be used to produce a high fidelity description of the distribution of rupture forces. This analysis is equally suitable for describing rupture forces in molecular and biomolecular contexts with a number of measurement techniques.

PACS numbers: 82.70.Dd, 83.80.Hj, 87.80.Ek, 87.80.Nj

It has been long known that the process of bond breaking is stochastic. Kramers' depiction of barrier hopping showed that the ever present thermal forces restoring equilibrium at molecular and near molecular scales result in a spectrum of bond lifetimes [1]. The observation of variable bond lifetimes and quantification of the mean time to first cross the barrier enabled development of transition state theory for predicting chemical reaction rates [2]. When an external force is used to lower the barrier maintaining the bond, the point at which the bond ruptures is also stochastic. There exists a distribution of rupture forces much in the same way there is a spectrum of equilibrium bond lifetimes [3–6]. This principle applies equally well to chemical bonds or physical bonds as demonstrated on the macromolecular scale in the unfolding of proteins [7, 8] and the unbinding of ligand-receptor pairs [9, 10].

We present a new means of measuring and analyzing rupture forces based on an ensemble average of trajectories of colloidal particles during the rupture process. This has broad relevance extending beyond the usual biophysical contexts. For instance, in out-of-equilibrium, colloidal materials such as attractive glasses and gels, there is a short-ranged, attractive potential which drives particle aggregation [11, 12]. Such materials possess a yield stress that relates to the fracturing of an ensemble of particle-particle bonds. We show that the rupture forces are statistically distributed much as in protein unfolding or ligand-receptor binding. The rupture force distribution is measured at the particle level while varying the depth of the short ranged potential. The short-ranged potential examined here presumably arises from a superposition of van der Waals attraction and screened electrostatic repulsion – the so-called DLVO interaction [13]. "Rupture" of a "bond" as commonly defined requires only that the attractive potential is deep relative to the thermal energy and narrow relative the scale of observation so that clear distinction between bound and unbound states can be made. The DLVO potential, like many colloidal interactions, possesses such qualities.

A dilute, aqueous suspension of colloidal particles (poly-methyl-methacrylate, PMMA, Bangs Laboratory PP04N, $a \approx 1.57\mu$m in diameter, zeta potential measured via electrophoresis of -41 ± 4 mV in 2 mM KCl, washed in ultra-pure water, centrifuged and decanted 5x to 20% strength) is destabilized through addition of the anionic surfactant (sodium dodecyl sulfate, SDS) at concentrations of 25, 35, 40, 50 mM. Two particles are trapped by time shared laser tweezers (a 4-W CW Nd:YAG laser, steered by perpendicular acousto-optic deflectors through a 63×, 1.2 NA water immersion objective). One trap is static while the other traces a reciprocating trajectory at a uniform rate [14, 15]. The addition of SDS attenuates the repulsive electrostatic barrier between particles and precipitates a secondary minimum in the interaction potential with a depth that depends on surfactant/salt concentration [13]. For PMMA in solutions of SDS at between 25 mM and 50 mM in concentration, the attractive potential is estimated to have a range less than 50 nm and a depth of $10\,k_BT$ to $50\,k_BT$ [16]. Statistical sampling of the rupture is achieved by subjecting the particle pair to numerous adhesion/rupture cycles (fig. 1).

The optical traps serve as linear force transducers. Consequently, the rupture force is proportional to the maximum displacement of the particle from the focus of the trap immediately preceding rupture. This displacement is measured using back-focal plane interferometry in which the laser light scattered from the trapped particle is collected and imaged onto a quadrant photodiode

*Shindel conducted the experiments while Swan was responsible for the proposed analysis
†Corresponding author: furst@udel.edu

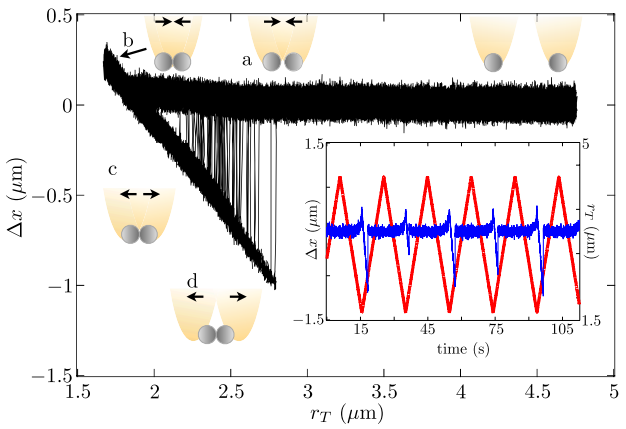

FIG. 1: An illustration of the experiment. Inset: Displacement of the particle from the static trap (blue, thin) and separation between optical traps (red, thick) as a function of time. The same quantities are plotted parametrically (black). The experimental process brings the particles together by decreasing the separation between the laser traps (a). When the particles come into contact, they experience a hard repulsion (b). Contact also bonds the particles so that when the traps are retracted, the particles do not immediately separate (c). Bond rupture results in rapid reduction of the displacement as the adhesive force binding the particles to one another dissipates (d). Accompanying the figure are cartoons depicting the relative positions of the particles and the traps throughout the cycle.

(QPD). The differential light intensity across the quadrants is linearly proportional to the displacement of a particle from the focus of the optical trap. The QPD directly measures particle displacements with a bandwidth exceeding 10 kHz. By time sharing the laser and coordinating the sampling of data from the QPD, the displacement of the particle in the static trap and the particle in the dynamic trap can be distinguished straightforwardly.

A parametric plot of particle displacement in the static trap, denoted Δx, versus separation between optical traps, denoted r_T, (fig. 1) shows all rupture events in a given experiment and reveals that the physical disassociation of colloidal particles is stochastic. Rather than having a singular, characteristic force value, there is a distribution of forces associated with escape from the secondary minimum. These experiments are also sensitive to non-contact forces. The positive displacement, prior to contact, in the profile shown in fig. 1 stems from an induced, optical dipole arising from time sharing the laser. The corresponding polarizations produce a long-ranged, but weak, repulsion [17]. This repulsion persists up to the point where the particles nearly contact at which point the particles are drawn into the DLVO secondary minimum and bonded tightly. They proceed to interact through the mutual repulsion provided by the residual electrostatic double layer.

The average particle trajectories on approach and retraction are depicted as a parametric plot of displacement of the static particle from the static trap, $\langle \Delta x \rangle$, versus the separation between the optical traps, r_T, in fig. 2 as well. Beyond the range of the DLVO and optical dipole interactions, the static particle resides strictly within its trap so that $\langle \Delta x \rangle \approx 0$. This assumes the trap moves slowly and hydrodynamic forces are negligible when particles are widely separated. However on approach (averages denoted with a subscript "A"), the repulsive optical dipole drives the static particle out of the trap focus so that $\langle \Delta x \rangle_A > 0$ until the DLVO secondary minimum is reached. On retraction (averages denoted with a subscript "R") , the minimum adheres the particles. While the particles are bonded the tweezers continue to separate at a constant rate. The displacement of the static particle from its trap grows linearly as $\langle \Delta x \rangle_R = g(r_T) = (a - r_T)/2$. This continues until the inter-particle bond ruptures and the static particle jumps to a trajectory analogous to its approach. A definition of adhesive contact diameter, a, is given by the first value of trap separation, r_T, at which $\langle \Delta x \rangle_A = \langle \Delta x \rangle_R$ when the short-ranged double layer repulsion acts. The rupture force is that exerted by the secondary minimum to maintain mechanical equilibrium in the moment before the rupture event occurs. This is also the force exerted by the optical tweezers and is proportional to the displacement of the particle from the center of the optical trap. High frequency measurement of the displacement is necessary to precisely sample this same moment.

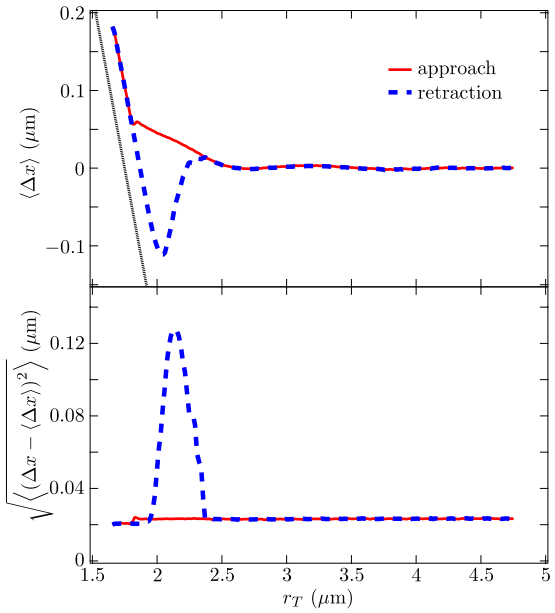

FIG. 2: The displacement of the static particle from the static trap through many cycles is averaged over many cycles at the same separation between traps. This is plotted parametrically against the separation between the optical traps. This data corresponds to an experiment with 35 mM SDS and a 1.5 pN/s loading rate.

The magnitude of fluctuation in particle position is inherently related to the work required to raster the particles along the applied trajectory. This quantity exhibits a notable hysteresis between approach and retraction (fig. 2). The variance in displacement is largely constant during approach but decrements slightly as the traps reach a separation that causes the particles' surface-to-surface distance to be commensurate with the width of the secondary minimum. Diminution of the fluctuations represents a reduction in free energy upon formation of the bond. In contrast, rupture is clearly a non-equilibrium process. The rise in fluctuations far outweighs the preceding reduction, and thus a large amount of energy is dissipated during bond rupture. This energetic landscape is akin to that for an irreversible, bimolecular reaction.

The trapped particles occupy one of two "states" in the retraction leg of the cycle: either the pair is bonded so that the displacement of the static particle from its trap grows linearly: $\Delta x = g(r_T)$ or the bond has ruptured and $\Delta x \approx \langle \Delta x \rangle_A$. The latter state may be justified when the optical traps are much stronger than the thermal energy so that the particle centers deviate little from the trap location when driven by Brownian motion alone. The fluctuations in the particle trajectories demonstrate aside from the adhered, pre-rupture state, the optical trap moves slowly enough that the particles maintain their equilibrium distribution (see fig. 2). Consequently, the probability of finding the static particle displaced by Δx from the static trap on retraction when the traps are separated by r_T is

$$P(\Delta x, r_T) = W(r_T)\delta\left(\Delta x - g(r_T)\right) + \left(1 - W(r_T)\right)\delta\left(\Delta x - \langle \Delta x \rangle_A\right),$$

where $W(r_T)$ is the probability of finding the pair of particles bound in the potential minimum when the traps are separated by r_T and $\delta(x)$ is the Dirac delta function. The rates at which the particles come together and are pulled apart are implicitly represented in this two-state model.

The average static particle displacement during retraction – the expectation value of Δx with respect to $P(\Delta x, r_T)$ – is $\langle \Delta x \rangle_R = \langle \Delta x \rangle_A + W(r_T)\left[g(r_T) - \langle \Delta x \rangle_A\right]$. The probability that the particles reside in the potential minimum when the traps are separated by r_T is then the ratio

$$W(r_T) = \frac{\langle \Delta x \rangle_R - \langle \Delta x \rangle_A}{g(r_T) - \langle \Delta x \rangle_A}.$$

Similarly, the probability of the particles escaping the potential well (rupturing) at r_T, is $L(r_T) = -dW/dr_T$. Here, $L(r_T)$, is the probability density of rupture events when the traps are separated by r_T. By basing the probability distribution on the difference between approach and retraction trajectories, the effects of the optical dipole have been eliminated entirely [17]. Contrast this with measuring the effect of the optical dipole in a control experiment (something we have done but do not show) and subtracting it manually from the measured rupture forces.

As the optical trap is merely a spring stretched a distance $(r_T - a)/2$ at the moment of rupture, a linear shift and rescale of the argument of $L(r_T)$ is all that is required to determine the distribution of rupture forces. For a Hookean spring force $f = k(r_T - a)/2$ with stiffness k, $\hat{L}(f) = (2/k)L(2f/k + a)$ is the probability density of rupture forces satisfying the normalization criterion that an integral of $\hat{L}(f)$ over all force is unity.

Notably, the average displacement of the static particle from the static trap, $\langle \Delta x \rangle$, on approach *and* retraction *together* encode the distribution of rupture forces. Therefore, hundreds of cycles of approach and retraction may be performed and through simple analysis a detailed probability distribution developed. This is far simpler than manually and individually scanning trajectories, attempting to determine when or where a rupture event occurred, calculating the rupture force and assembling a histogram of these forces – trivial for a few dozen trajectories but challenging for more than that. Significantly, the statistics of even small rupture forces are incorporated into the preceding method while the manual approach fails to identify rupture events in which the forces are not many times the thermal energy.

We perform rupture experiments with between 150 and 220 approach/retraction cycles. When the particles are widely separated, the power spectral density of the displacement of the static particle from the static trap center is Lorentzian and can be fit to determine the trap stiffness. Therefore, the stiffness of the optical trap is characterized by the spectrum of fluctuations in the static particle position. The stiffness ranged from 8 to 31 pN/μm to accommodate deeper secondary minima at higher SDS concentrations. While the particles are bonded but the laser tweezers are moving (together or apart), the quadrant photodiode measures a linear change in voltage. When plotted against the separation between the traps, the slope of this line characterizes the sensitivity (displacement to voltage ratio) of the photodiode. A typical value was 300 nm/V which provides a spatial resolution of 1.5 nm displacement or a force resolution of ~ 10 fN.

The probability of finding the particles bonded when the laser tweezers exerts a force f on retraction, $W(r_T) = W(2f/k + a)$ is plotted in fig. 3. In that same fig., we plot the corresponding probability density of rupture forces. It has been observed that the rate of loading affects the distribution of rupture forces [3–5]. The experiments in fig. 3 were performed with the speed of approach and retraction fixed at 0.24 μm/s. Because the stiffness of the laser trap was adjusted to accommodate strong adhesion of particles on increasing SDS concentration, the rate of loading was not controlled and varied from 2 pN/s at 25 mM SDS to 8 pN/s at 50 mM SDS. We repeat the experiment at 35 mM SDS and vary the loading rate (see fig.

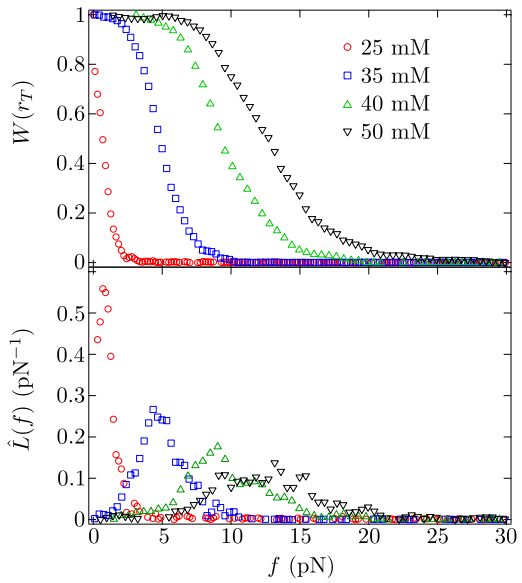

FIG. 3: The probability of a bond being un-ruptured $W(f)$ and the probability density of rupture forces $\hat{L}(f)$ at a given loading f are plotted for various SDS concentrations.

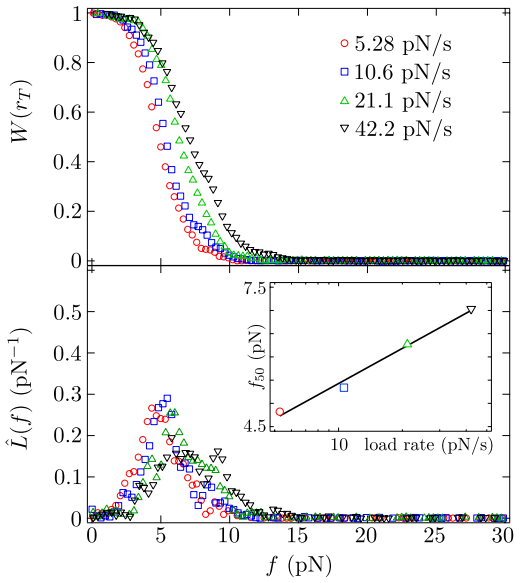

FIG. 4: The probability of a bond being un-ruptured $W(f)$ and the probability density of rupture forces $\hat{L}(f)$ at a given loading f are plotted for various load rates for 35 mM SDS. The inset plots the point at which the cumulative force distribution reaches 50%, denoted f_{50}, as a function of load rate. The dashed line indicates a logarithmic fit.

4). The loading rate may be changed by varying either the rate of relative motion or the stiffness of the optical traps. We chose the former. In the limit that motion of the trap is slow relative to the thermal relaxation rate *and* the trap is stiff relative to the thermal stress, these approaches are equivalent. These conditions describe the linear response limit, and both are satisfied in the present experiments.

In fig. 4, the concentration of SDS is 35 mM, and the interaction potential between the particles is fixed. Kramers' barrier hopping theory predicts the rate of escape from a fixed potential well. The logarithmic dependence on loading rate is a consequence of this theory in the limit that the load aiding escape from the potential well grows linearly in time [1, 3]. Here, we vary the rate of separation of the traps while keeping the trap stiffness fixed and find that the rupture force at which half the bonds breaks, denoted f_{50} and given by $W(f_{50}) = 1/2$, scales precisely as Kramer's theory predicts, with the logarithm of the loading rate (see the inset of fig. 4). The loading rate is implicitly represented in the two-state model proposed herein. The inset of fig. 4 shows that such a model reproduces the result expected from theory and observed in past experiments [3–5]. When the SDS concentration is varied, there is no such theoretical dependence on loading rate since the amount of salt in solution changes the interaction potential.

The broad statistical distribution for rupture forces reveals that thermal fluctuations play an inescapable role in the bond breaking process. The balance of mechanical forces makes the bond susceptible to breaking by Brownian impulse. We neglected the effect of hydrodynamic interactions in this balance because throughout most of the cycle relative particle motion is slow and hydrodynamic forces are weak. While the particles are separated the ratio of the rate of relative motion to the rate of particle diffusion (called the Péclet number) is less than 10^{-1}. The particles are equilibrated when widely separated. However, just after rupture the particles are subject to strong hydrodynamic forces – the Peclet number is nearly 10^3. Rupture is a highly non-equilibrium event.

The analytical methodology developed herein is widely applicable and ought to be adopted in future measurements of rupture forces. Expressing the probability of finding the particles bonded, W based on an ensemble average of approach and retraction trajectories may be cast in the contexts beyond colloidal interactions and optical tweezers. For instance, with AFM, on retraction, the deflection of the cantilever is either changing linearly while in the bonded state with probability W or following the approach trajectory with probability $1 - W$. The fraction of bonds at each cantilever displacement can be calculated directly from these averaged trajectories.

We are grateful for funding from International Flavors and Fragrances and NASA (grant no. NNX10AE44G).

[1] H.A. Kramers. *Physica*, 7(4):284–304, 1940.
[2] P. Hanggi, P. Talkner and M. Borkovec. *Reviews of Modern Physics*, 62(2):251–341, 1990.

[3] E. Evans and K. Ritchie. *Biophys. J..*, 72:1541–1555, 1997.
[4] E. Evans. *Faraday Disc.*, 111:1–16, 1999.
[5] E. Evans. *Annu. Rev. Biophys. Biomol. Struct.*, 30:105–128, 2001.
[6] D. Viehman and K.S. Schweizer, *J.Chem. Phys.*, 128:084508, 2008.
[7] H. Dietz, F. Berkemeier, M. Bertz and M. Rief. *Proc. Nat. Acad. Sci.*, 103(34):12724–12728, 2006.
[8] M.J. Buehler and Y.C. Yung. *Nat. Mat.*, 8:175–188, 2009.
[9] J. Fritz, A.G. Katopodis, F. Kolbinger and D. Anselmetti. *Proc. Nat. Acad. Sci.*, 95:12283–12288, 1998.
[10] W. Hanley, O. McCarty, S. Jadhav, Y. Tseng, D. Wirtz and K. Konstantopoulos. *J. Bio. Chem.*, 278(12):10556–10561, 2003.
[11] C.J. Dibble, M. Kogan and M.J. Solomon. *Phys. Rev. E*, 74:041403, 2006.
[12] K. Pickrahn, B. Rajaram and A. Mohrz. *Langmuir*, 26(4):2392–2400, 2010.
[13] W.B. Russel, D.A. Saville and W.R. Schowalter. Cambridge University Press, Cambridge, 1989.
[14] A. Ashkin and J.M. Dziedzic. *Science*, 20:1517–1520, 1987.
[15] A. Ashkin, J.M. Dziedzic and T. Yamane. *Nature*, 330:769–771, 1987.
[16] J.P. Pantina and E.M. Furst. *Langmuir*, 20:3940–3946, 2004.
[17] J.C. Crocker, J.A. Matteo, A.D. Dinsmore, and A.G. Yodh. *Phys. Rev. Lett.*, 82(21):4352–4355, 1999.